An Evaluation of the Feasibility of Several Industrial Wastes and Natural Materials as Precursors for the Production of Alkali Activated Materials

O. Alelweet, S. Pavia

Abstract—In order to face current compelling environmental problems affecting the planet, the construction industry needs to adapt. It is widely acknowledged that there is a need for durable, high-performance, low-greenhouse gas emission binders that can be used as an alternative to Portland cement (PC) to lower the environmental impact of construction. Alkali activated materials (AAMs) are considered a more sustainable alternative to PC materials. The binders of AAMs result from the reaction of an alkali metal source and a silicate powder or precursor which can be a calcium silicate or an aluminosilicate-rich material. This paper evaluates the particle size, specific surface area, chemical and mineral composition and amorphousness of silicate materials (most industrial waste locally produced in Ireland and Saudi Arabia) to develop alkali-activated binders that can replace PC resources in specific applications. These include recycled ceramic brick, bauxite, illitic clay, fly ash and metallurgical slag. According to the results, the wastes are reactive and comply with building standards requirements. The study also evidenced that the reactivity of the Saudi bauxite (with significant kaolinite) can be enhanced on thermal activation; and high calcium in the slag will promote reaction; which should be possible with low alkalinity activators. The wastes evidenced variable water demands that will be taken into account for mixing with the activators. Finally, further research is proposed to further determine the reactive fraction of the clay-based precursors.

Keywords—Reactivity, water demand, alkali-activated materials, brick, bauxite, illitic clay, fly ash, slag.

I. INTRODUCTION

IT is widely acknowledged that climate change adversely affects earth and endangers human and animal life. Economic losses due to climate change in Europe amounted to approximately EUR 453 billion between 1980 and 2017 [1], and annually, $2,245 billion losses are attributed to climate-related disasters [2].

PC is the most widely-used engineering material in the world, and the world demand is projected to rise by 5.2% during 2019-2024 [3]. To produce one ton of cement approximately one ton of carbon dioxide is projected to the atmosphere [4]. Moreover, cement production consumes significant natural resources, as 1.6 tons of raw materials are required to produce 1 ton of cement [5]. The forecasted increase in world demand (5.2%) will raise emissions and resource consumption significantly. Therefore, there is a need for durable, high-performance, low-greenhouse gas emission binders that can be used as alternatives to PC to lower the environmental impact of construction.

AAMs are considered a more sustainable alternative to PC products. They are produced at lower cost than PC, with low CO_2 emissions and low raw material and fossil fuel consumption, with energy savings up to 60% on production [6]. Alkali activated (AA) binders result from the reaction of an alkali metal source and a silicate powder or precursor which can be a calcium silicate or an aluminosilicate-rich material. AAMs were patented in 1958 and used in construction in 1960 in USSR; and precast products using AA cements are widespread in Eastern Europe, Finland and France [6].

This paper studies the physical properties and composition of silicate materials locally produced (in Ireland and Saudi Arabia). It evaluates the feasibility of using these silicates, as precursors, to develop alkali-activated binders and create sustainable materials that can replace PC products in specific applications. The silicate precursors include recycled ceramic brick, bauxite, illitic clay, fly ash and metallurgical slags. Some of them are waste that would otherwise end in landfills.

II. MATERIALS

The silicate materials evaluated as precursors include illitic clay, recycled ceramic brick, fly ash, metallurgical slag and bauxite.

A. Illitic Clay

A Tertiary marly clay from the Cormey quarry in County Cavan, Ireland, was used in this research. The mineral composition includes clay minerals (57%) and non-clay minerals consisting of quartz (26%), calcite (7.5%), feldspar (4%), goethite (1%), hematite (4%) and rutile (0.5%), and the clay fraction consists of illite (28%), chlorite (15%), smectite (5%), muscovite (4%) and fireclay (5%) [7].

B. Recycled Ceramic Brick

Crushed brick fabricated using the illitic clay above fired at 1030 °C by Kingscourt Brick Ltd. was also evaluated as a precursor. The bricks are extruded, wire-cut and fired in a tunnel kiln, following the production methods at Kingscourt Brick. Defective bricks with chippings, efflorescence or cracks are crushed and recycled on site.

Omar Alelweet is with Department of Civil Engineering, Trinity College Dublin, College Green, Dublin 2, Ireland (phone: 353- 896 1000; e-mail: alelweeo@ tcd.ie).

Sara Pavia is with the Department of Civil Engineering, Trinity College Dublin, College Green, Dublin 2, Ireland (e-mail: PAVIAS@tcd.ie).

C. Metallurgical Slag

A vitreous material formed by rapid cooling of a melt of iron ore in a blast furnace, known as ground granulated blast furnace slag (GGBS) was evaluated as precursor. GGBS usually consists of at least two thirds by mass of glassy slag, showing hydraulic properties when suitably activated [8]. It is widely used as partial PC replacement around the world. The GGBS in this study is produced in Ringsend, Dublin, with raw molten slag imported from Europe. Manufacturing produces 40 kilos of CO_2 per ton of GGBS but this is offset by carbon credits [45].

D. Fly Ash

Fly ash (FA) from a coal burning power plant in Moneypoint, Ireland is also used as a precursor. Due to their particle size distribution, chemical composition, generally spherical particle shape and low cost, FAs have been widely used as a supplementary cementitious material in concrete. Several FAs have been used by former authors for the production of AAMs. FA is probably the precursor most widely used to produce AA binders with results even commercialised in 1997 as a product known as Siloxo, used to produce ready-mix concrete and a range of pre-cast products from both Class F and Class C FA [9].

E. Bauxite

The bauxite is quarried by the Saudi Arabian mining company Ma'adem at Al Ba'itha, in the northern AL Qassim province. The mine's estimated production is 4 million tonnes per year, and the aluminium ore extracted used in high quality steel [10].

III. METHODS

A. Particle Size of the Precursors

The bricks and bauxite were ground for 3-4 minutes. Grinding was performed using a TEMA T100 Disc Mill (790 RPM; max sample 150 g). The bauxite was previously crushed with a jaw crusher to reach a particle size of 6-8 cm required for the ball mill. The remaining precursors did not require any processing. The particle size distribution was measured by laser diffraction using a Mastersizer 2000, composed of a Mastersizer 2000 unit; a Hydro 2000G wet dispersion and an Autosampler 2000 units. This method measures the angular distribution and intensity of the light by particles in suspension and utilises the Mie theory of diffraction in the prediction of laser particle size results. Statistics (D-Values) were applied to understand the particle size distributions whereby the distribution width is defined with three values on the x-axis: the D10, D50 and D90. The D50 (median) is the diameter where half of the population lies below this value. Similarly, 90% of the distribution lies below the D90, and 10% of the population lies below the D10.

B. Particle Density

The densities were measured according with EN 196-6 [11]. This property is important because it is closely related to the strength and porosity of the resultant AAMs. The strength of AAMs (in particular geopolymers) has been related to their density and porosity. In general, low porosity, high density and fine-grained microstructure contribute to high strength [12]. Some precursors produce lower densities than PC pastes. For instance, the bulk density of metakaolin geopolymers is reported to range between 1.20 and 1.80 g/cm^3; and coal FA geopolymers range between 1.40 and 1.80 g/cm^3 [13], [14]. In contrast, the density of PC paste is usually over 1.80 g/cm^3 [15].

C. Specific Surface Area

Surface chemistry is essential on the alkali activation process. Therefore, the specific surface area of the precursors determines their reactivity. The specific surface area was measured with a Quantachrome Nova 4200e and the BET method which records the specific surface area based on the physical adsorption of gas molecules by the precursors. The Brunauer–Emmett–Teller (BET) theory correlates the physical adsorption of gas molecules on a solid surface with the specific surface area of the particles.

D. Chemical and Mineral Composition and Amorphousness

Composition and amorphousness (amount of vitreous material) are essential as they control reactivity. The chemical composition was determined by XRF analysis, with an Epsilon 4 energy dispersive X-ray fluorescence (EDXRF) spectrometer. The results are reported as percentage by oxides. The mineral composition was determined with an X-Ray Diffraction (XRD) machine including a PW1050/80 goniometer and a PW3313/20 Cu k-alpha anode tube. Measurements were taken from 3 to 60 degrees (2θ) and the detection limit is 5%. An indication of the amorphousness of the precursors was provided by assessing the wide peak at c.20 degrees (2θ) which (despite not being accurately measured) correlates with the vitreous character of the silicates [16].

E. Loss on Iignition

The loss on ignition (LOI) was measured at 450 and 1000 °C to determine the carbon and carbonates content by thermal decomposition. The percent LOI is calculated from the difference in weight.

F. Workability by Initial Flow: Water Demand of the Precursors

The amount of water required for the precursor to provide a suitable workability for handling and placing was measured with the initial flow diameter test using a flow table. The flow diameter was selected according to EN 1015-3 [17], and the water required for each of the silicate materials to reach this flow is recorded. The water demand of the precursors is essential as it affects drying, setting and hardening and, if too high, it can cause shrinkage fracturing or strength loss by increased porosity.

IV. RESULTS AND DISCUSSION

A. Particle Size, Density and Specific Surface Area

It is well known and widely accepted that, in general,

chemical reactivity increases at small particle sizes and high surface areas. Similarly, the alkaline activation of a precursor is usually enhanced at small particle sizes and high surface areas [9], [18]. The particle density has been related to the strength and porosity of the resultant AAMs. In general, high density, low porosity and a fine-grained microstructure contribute to high strength [12].

According to the particle size parameters measured, the clay and GGBS are the finest with medians of c.8 and 11 microns respectively (the size of half of the particles is below these diameters). The clay contains the finest particles amongst all precursors (10% are under 1.7 microns) while the coarsest particles of all precursors are found in the brick. However, the clay contains a much wider range of particle sizes than the GGBS whose particles are more consistent in size (90% under 31 microns). The particles in the brick, clay and bauxite span over a wider size range than the FA and GGBS.

The clay has the highest specific surface area and particle density. The clay's surface area is much greater than any of the other precursors except for the bauxite (c.25% lower specific surface area than the clay). The clay and bauxite have the greatest surface areas by far. However, the clay is finer. The high specific surface area should enhance the rate and intensity of the alkaline activation reaction. The bauxite and the recycled brick are the coarsest. However, as aforementioned, the bauxite has a great specific surface area (highest of all except for the clay) which means that the bauxite particles are porous. GGBS is the finest but its surface area is the lowest, similar to that of limestone cement (CEM II). This indicates that the GGBS particles are non-porous.

The clay particles are the densest closely followed by the bauxite (2.65 vs 2.43 mg/m^3). The GGBS particles are the lightest (1.80) while the brick and the FA follow at 2.18 and 2.28 mg/m^3 respectively.
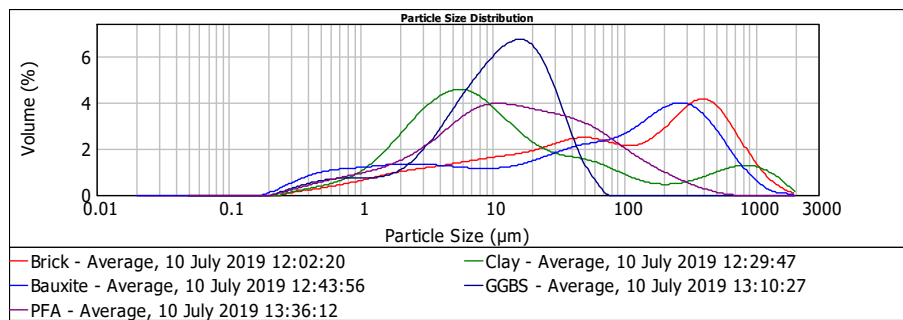

Fig. 1 Particle size distribution of the silicate precursors by laser grading

TABLE I
SUMMARY OF RESULTS OF SPECIFIC SURFACE AREA, PARTICLE SIZE AND DENSITY OF THE PRECURSORS COMPARED WITH CEM II /A-L 32, 5N (6-20% LIMESTONE AND 5% MINOR ADDITION)

	specific surface area (SSA) m^2/g	specific surface area (SSA) m^2/kg	particle density mg/m^3	Particle Size				Rating	
				mean μm	D90 μm	D50 μm	D10 μm	Fineness –finest on top	SSA-greatest on top
Clay	23.99	23990	2.65	6	0.20 to 2000 422.26	8.64	1.79	clay	*clay*
Brick	8.23	8280	2.18	15	0.25 to 3000 612.87	85.81	3.26	GGBS	*bauxite*
Bauxite	17.92	17920	2.43	300	0.10 to 3000 463.94	74.1	1.22	FA	brick
FA	6.50	6500	2.28	15	0.20 to 650 100.63	14.96	1.95	bauxite	FA
GGBS	1.95	1950	1.80	18	0.25 to 75 31.62	11.67	2.35	brick	GGBS
CEM II	1.88	1880	-		-			-	CEM II

B. Workability and LOI

Workability is an essential criterion that must be taken into consideration in the design of AAMs [15], [19], [20]. According to Feng and Clark [21], the water requirement is influenced by the fine particle fraction and, the LOI having an impact on water demand owing to the absorption of water molecules by porous carbon particles.

The carbon content is also important in AAMs as it absorbs moisture lowering reactivity and workability. Previous authors have found carbon to adversely affect the compressive

strength of AAMs [22]. In AAMs, the carbon particles absorb the activator solution, thus obtaining a workable mixture requires a volume of activator solution far beyond what is necessary to activate the source material. This can result in unreacted and partially reacted precursor particles in the mix, leading to lower compressive strength [23]-[25].

GGBS shows the worst workability (highest water demand at 36%), followed by the recycled brick and the bauxite at c.30%. The highest water demand of the GGBS is likely due to its fineness and to the hydraulic nature of some of its

components (calcium silicates) binding water molecules as they hydrate. The FA displays the best workability (lowest water demand at 15%) probably due to the spherical shape of its particle constituents. It was expected that the FA would enhance workability due to the characteristic shape of its particles. According to previous authors, FA-based AA materials are of particular interest as they can display superior workability with less water than other precursors such as metakaolin which may result in improved mechanical properties [26].

It was expected that the clay, bauxite and brick would present a high-water demand due to the nature of their layered, clay mineral components and the typical high hygroscopicity of clay-based ceramics. The higher water demand of the clay with respect to the FA was evidenced in alkali activation by former authors [27]. Binders synthesised from the alkali-activation of metakaolin require large volumes of water to create workable pastes [26]. However, despite their water demand, hardened metakaolin based inorganic polymers can exhibit comparable or superior mechanical properties to PC [28].

TABLE II
WATER DEMAND TO REACH A GIVEN INITIAL FLOW DIAMETER AND LOI

	water/precursor (%)	Flow diameter (mm) [17]	LOI (%)	
			450 °C	1000 °C
Clay	27	170	0.21 0.05[a]	5.10 6 - 7[a]
brick	33	174	11.49	21.75
Bauxite	30	170	0.30	1.10
FA	15	170	1.67	4.92
GGBS	36	170	0. 41	-0.77
CEM II	24	173	-	-

[a][7]

All of the silicate precursors have low carbon contents (0.21-1.67%) except for the recycled ceramic bricks (11.49%). The carbon content here is secondary due to exposure, as the bricks were left outdoor for months before they were crushed and recycled. Given the presence of carbonate in the raw clay and the outdoor exposure, the high LOI of the brick at 1000 degrees is due to the presence of both primary and secondary carbonates.

As FA and GGBS have been used as a blend in cement for

decades, the influence of carbon in their reactivity has been previously studied. Ha et al. [29] indicate that FA containing 8% of unburned carbon could accelerate the corrosion of steel reinforcement. According to EN 196-2 [30] and EN15167-1 [8], the maximum carbon allowed for GGBS is ≤ 3 %. In this study, the carbon content is negative (-0.77%). Therefore, the GGBS meets the standards; however, the negative value indicates that the GGBS absorbed some moisture during testing.

C. Composition and Amorphousness

As mentioned, the crystallinity vs. amorphousness of the precursor is important because it determines dissolution/hydrolysis of the mineral components and thus reactivity. The dissolution of minerals and glasses has been studied for many systems, including silicate and aluminosilicate glasses under highly alkaline conditions since the 60s up to recently [31]. It is widely accepted that the reactivity of a silicate material increases proportionally with the amount of amorphous content. Previous authors state that crystalline phases (e.g. quartz and mullite in FA) are unreactive because the rate at which they react in alkali-silicate solutions is extremely slow when compared with amorphous materials [26], [32], [33]. Other researchers agree that even after long cure, the crystalline phases are observed in identical amounts by XRD [34].

According to previous authors, the amorphous character of the precursors correlates with the size of the XRD trace broad peak at around 20 degrees of 2θ [32]. According to this, the FA and GBBGS are mostly and totally amorphous respectively (Table III). However, in the clay-based materials, the amorphous character is not clear as the peak becomes concealed by the total clay reflection (d-spacing = 4.48 Å at 2θ = c.20 degrees), and overlapped by the illite/muscovite reflection, while in the bauxite, the peak is concealed by the 4.46, 4.37, 4.29 Å reflections corresponding to kaolinite ($Al_2O_3 \cdot 2SiO_2 \cdot 2H_2O$), gibbsite $Al(OH)_3$ and gypsum ($CaSO_4 \cdot 2H_2O$) respectively (Table III).

As the amorphousness peak was concealed, in order to establish the likely reactivity of the clay-based materials, the mineral transformations in the clay during firing were studied (Table IV).

TABLE III
MINERAL COMPOSITION AND AMORPHOUSNESS DETERMINED WITH XRD [35]

	Rate of amorphousness (0-5)	Mineralogical composition			
		Major >40%	*Subsidiary 40-15%*	*Minor 15-7%*	*Traces < 7%*
Illitic clay (raw)	Peak concealed by the total clay reflection d-spacing = 4.48 Å	quartz	chlorite/smectite muscovite/illite,	calcite feldspar (Ca plag)	hematite
Illitic clay fired at 600 °C	Peak concealed by the total clay reflection (4.48 Å)	quartz, feldspar (anorthite)		calcite, muscovite/ilite	
Brick (clay at 1030 °C)	(1-2) Crystalline	Quartz	K feldspar	gehlenite	hematite
Bauxite	Peak concealed by 4.46, 4.37, 4.29 Å (kaolinite, gibbsite and gypsum) reflections	-	gibbsite boehmite kaolinite	gypsum anatase clinoenstatite	-
GGBS	(5) Totally amorphous		No crystalline fraction		
FA	(3) Intermediate	Amorphous phase	quartz		mullite

In the raw clay, the total clay peak (4.48Å) is clearly visible and, as aforementioned, conceals the amorphous hump (2θ = 20). At 600 °C, this reflection becomes sharper and more intense which is interpreted as the partial transformation of illite into a greater crystallinity phase (muscovite). In addition, at 600 °C, the chlorite/smectite increases its first reflection (14Å) while the others either reduce significantly (7.09Å) or disappear. However, at higher temperature (1030 °C), both the clay and the chlorite/smectite reflections have disappeared, as well as the carbonate, indicating that these phases have decomposed and their Ca, Al and K become part of the new-formed, high-temperature phases potassium feldspar - $KAlSi_3O_8$- and gehlenite - $Ca_2Al(AlSiO_7)$-, Table IV. These mineral transformations agree with former authors who claim that, in an illitic calcareous clay, illite-mica begins to transform at over 600 °C to disappear at 800 °C while chlorite slightly increases (400-600 °C) to disappear before 750 °C [36], [37]; and calcite ($CaCO_3$) decomposes at approximately 750-850 °C in a natural clay, with calcium silicates (gehlenite, diopside/wollastonite) and feldspar appearing in the range 850-900 °C [38]. In the raw clay investigated, the rather high illite content indicates a high potassium content which has likely acted as a flux enhancing sintering, so that transformation may have taken place at slightly lower temperatures. From these results, the main clay mineral components of the raw clay increase crystallinity up to 600 degrees to later decay to high temperature, crystalline, calcium aluminum silicates like gehlenite and feldspar. Therefore, it seems that the illitic clay increases crystallinity as temperature rises which would make it less reactive. On the contrary, the high kaolinite content of the bauxite (ranging between 15 and 40% - Table III) suggests that the bauxite is likely to significantly increase its reactive, amorphous fraction on thermal activation. The removal of the chemically bonded hydroxyl ion, at controlled temperature, collapses the kaolinite structure producing amorphous metakaolin [39].

TABLE IV
MINERALOGICAL TRANSFORMATION OF THE ILLITIC CLAY ON FIRING AT 600 AND 1030 °C

Material	Peak at 2θ = 20 degrees	Chlorite/smectite d-spacing c.14Å	Illite/Muscovite d-spacing = 10.04Å K$_{0.65}$ Al$_2$ [Al $_{0.65}$Si $_{3.35}$O $_{10}$] (OH)$_2$	Chlorite d-spacing = 7.09Å	Silicates		Carbonates
					Calcium aluminosilicates	Feldspar	Calcite - CaCO$_3$
Illitic clay (raw)	Concealed by the total clay reflection d-spacing = 4.48Å	Present at very low intensity	Significant at 10.04Å (muscovite low/illite)	Clearly present	Not Detected	Plagioclase	CaCO$_3$ Clearly present
Fired at 600 °C	4.48Å peak sharper and slightly more intense	Sharper and much more intense	Shifts to 9.99 Å and significantly increases intensity/sharpness	Lowers intensity	Not Detected	Calcium plagioclase	Lowers intensity
Fired at 1030 °C	Disappears	Disappears	Disappears	Disappears	Gehlenite Ca$_2$Al(AlSiO$_7$)	Potassium feldspar KAlSi$_3$O$_8$	Disappears

According to the chemical composition results (Table V), the FA has a low Ca content (< 5 wt% CaO). Therefore, it can be classified as a low Ca FA (Class F according to ASTM C618), as the Ca is very low (< 10%) and the $SiO_2 + Al_2O_3 + Fe_2O_3$ content is over 70%.

Table VI compares the chemical composition of the FA in this research with the requirements in Garcia-Lodeiro et al. [40], EN 197-1 [41] and EN450-1 [42]. As it can be seen from Table VI, the FA complies with the chloride and sulphate (SO_3) content requirements in EN 450-1 (shall not be greater than 0.1% and 3.0% by mass respectively) which classifies FAs according to their suitability for use as type II additions in PC concrete. Also, the FA complies with the EN 197-1 [41] requirements on the content of magnesium oxide (MgO ≤ 4.0% by mass); the total phosphate ($P_2O_5 ≤ 5.0\%$) and the $SiO_2 + Al_2O_3 + Fe_2O_3$ content (over 70%), and it probably complies with the EN 197-1 [41] requirements on the amount of reactive silica (it shall not be less than 25% by mass), Table VI. Finally, the FA also meets the requirements for use in the production of AA cements set by Garcia-Lodeiro et al. [40], Table VI. It is not known exactly how much of the total SiO_2 (60%) is reactive. However, approximately 50% of the FA is amorphous therefore a significant fraction of the total silica is reactive.

The slag complies with the European standard requirements for the use of GGBS in concrete, mortar and grout slag [8] in Table VII, as it consists of at least 2/3rd by mass of the sum of magnesium oxide (MgO), silicon dioxide (SiO_2) and calcium oxide (CaO), the remainder is aluminium oxide (Al_2O_3) (with small amounts of other compounds), and it contains no added materials.

The GGBS can be classified as a Ca-rich precursor (Ca = 35-40%). It contains network forming elements (Si, Al, Mg) which when the slag dissolves in the alkali solution should provide network-forming anions $(SiO4)^{4-}$, $(AlO4)^{5-}$ and $(MgO4)^{6-}$ [40]. In addition, the slag is totally vitreous and no crystalline phases were detected with XRD (Table III). Slag reactivity in alkaline activation depends largely on the vitreous phase content therefore, the slag should be active.

Garcia-Lodeiro et al. [40] include further requirements for slags to be apt for use in AA systems. Amongst these, the slag should be pH-basic (i.e. have CaO+MgO/SiO$_2$ ratio > 1). The slag of this research has a ratio of 1.56; therefore it qualifies as active in an AA system (Table VII). This significant basicity will likely result in shorter setting times regardless of the activator [43] and can also enhance strength [44].

A further requirement is that the specific surface should be 400-600 m^2/kg (or not be less than 275 m^2/kg [8] to be considered adequate for PC substitution). This GGBS has a greater fineness at 1950 m^2/kg. This high specific surface should increase significantly the rate and the intensity of the alkaline activation reaction.

TABLE V
CHEMICAL COMPOSITION OF THE SILICATE PRECURSORS BY XRF

	SiO₂	Al₂O₃	CaO	Fe₂O₃	Na₂O	K₂O	MgO	P₂O₅	SO₃	Cl	TiO₂	MnO	CuO	SrO	ZrO₂
GGBS	31.71	10.83	44.9	0.51	0.03	0.71	7.50	0.42	2.08	0.03	0.95	0.17	0.00	0.07	0.05
GGBS[b]	34.14	13.85	39.27	0.41	0	0.26	8.63	-	2.43	-	0.54	0.25	-	-	-
GGBS mean	*32*	*12*	*42*	*0.45*	*0.03*	*0.5*	*8*	*0.42*	*2.2*	*0.03*	*0.75*	*0.2*	*0*	*0.07*	*0.05*
Clay	55.84	19.76	4.92	8.71	0.00	5.63	3.05	0.60	0.04	0.04	1.17	0.12	0.00	0.03	0.05
Clay[a]	57-59	15-18	3.7-4.1	4.7-6.3	0.3-0.5	4.60	1.7-2.4	-	0.1-0.6	-	0.80	-	-	-	-
Clay mean	*58*	*18*	*4*	*6*	*0.2*	*5*	*2.8*	*0.6*	*0.2*	*0.04*	*1*	*0.12*	*0*	*0.03*	*0.05*
FA	53.40	21.18	4.14	9.99	0.70	3.24	1.86	0.84	2.67	0.04	1.35	0.07	0.03	0.12	0.05
FA[b]	65.32	24.72	0.94	4.84	-	1.37	0.68	0.37	0.37	-	0.91	-	-	-	-
FA mean	*59*	*23*	*3*	*7*	*0.4*	*2*	*1*	*0.5*	*1.4*	*0.04*	*1*	*0.07*	*0.03*	*0.12*	*0.05*
brick	55.40	18.73	6.85	8.18	0.20	5.37	2.97	0.59	0.24	0.03	1.06	0.17	0.02	0.03	0.04
bauxite	26.82	54.03	2.48	6.02	0.00	0.23	0.00	0.59	2.89	0.26	5.63	0.01	0.03	0.16	0.38
bauxite[a]	14.85	52.53	1.15	4.00	0.19	0.06	0.13	0.13	1.57	-	4.78	<0.01	-	-	-
bauxite mean	*21*	*53*	*2*	*5*	*0.1*	*0.1*	*0*	*0.4*	*2*	*0.26*	*5*	*0.01*	*0.03*	*0.16*	*0.38*

[a] results by the producers and [b] results by former authors [35].

TABLE VI
COMPOSITION OF THE FA IN THIS RESEARCH COMPARED WITH THE REQUIREMENTS IN GARCIA-LODEIRO ET AL. [40], EN 197-1 [41] AND EN 450-1 [42]

	FA Moneypoint	Garcia-Lodeiro et al. [40]	EN 450-1 [42]	EN 197-1 [41]
Unburned C	1.67	< 5%	-	-
Fe₂O₃	4.8%	≤ 10%	-	-
CaO	0.9%	≤ 10%	-	-
Vitreous phase content	40-60%	> 50%	-	-
SiO₂ reactive	Total 59% (including c. 50% total amorphous fraction)	> 40%	-	≥ 25 %
SiO₂ (reactive)/Al₂O₃ (reactive)	-	> 1.5	-	-
Particle size	90% < 100 microns	80-90% < 45 microns	-	-
chloride	0.04	-	≤ 0.1 %	-
sulphate (SO₃)	1.4	-	≤ 3.0 %	-
MgO	1	-	-	≤ 4.0 %
P₂O₅	0.5	-	-	≤ 5.0 %
SiO₂ + Al₂O₃ + Fe₂O₃	59+23+7 = 89	-	-	> 70%

TABLE VII
COMPOSITION OF THE GGBS IN THIS RESEARCH COMPARED WITH THE REQUIREMENTS IN GARCIA-LODEIRO ET AL. [40] TO QUALIFY AS ACTIVE IN AN AA SYSTEM AND THE EN 15167-1 [8] REQUIREMENTS TO QUALIFY AS PC SUBSTITUTION

	GGBS Ringsend	Garcia-Lodeiro et al. [40]	EN 15167-1 [8]
CaO + MgO/SiO₂	42+8 / 32 = 1.56	> 1 (pH-basic)	>1
CaO + MgO + SiO₂	82%	-	≥ 2/3 (≈ 66%)
Al₂O₃	12%	-	Reminder + small amounts of other
specific surface area	1950 m²/kg	400-600 m²/kg	Fineness: SSA[a] ≥ 275 m²/kg
Unburned C	0.40%	-	≤ 3% 3.5% single result limit value
chloride	0.03%	-	≤ 0.10%
sulphate (SO₃)	2.20%	-	≤ 2.50%
MgO	8%	-	≤ 18%

[a] SSA = Specific surface area

V. CONCLUSION

The results indicate that the silicate precursors are reactive and comply with requirements by building standards and previous authors for use as supplementary cementitious materials in PC and/or as precursors in AAMs. However, further research is required to ascertain the amorphous, reactive fraction of the clay-based precursors. The amorphousness of the clay-based materials is not clear, as peaks are overlapped and concealed by crystalline phases. Therefore, the amount of vitreous phase will be further studied with chemical attack and devitrification methods according to the standards.

The results also revealed that the Saudi bauxite contains significant kaolinite which is likely to become amorphous on thermal activation. Further research will apply thermal treatment to the bauxite, to remove the chemically bonded hydroxyl ion and collapse the kaolinite structure and produce amorphous metakaolin activating its AA reaction.

According to the chemical composition results, the only high calcium precursor is the slag, all the other being low calcium. In addition, with the exception of the bauxite (with high alumina content- 53%), all the precursors show a medium aluminium content (12-23%). The chemistry of the slag

suggests that it does not need an eminently alkaline activator to produce an AA binder. Therefore, the slag will be activated with either alkaline silicates or alkali hydroxides of low concentration.

The water requirement and LOI results suggest that, rather than the absorption of water molecules by porous carbon particles, the water demand is influenced by the fineness and nature (porosity, layered structure) of the particles (the FA has the greatest carbon content and yet the lower water demand while the GGBS –finest-, bauxite and clay have the highest water demand).

As the water demand of the precursors to achieve a specific workability is different, obtaining a workable mixture will require different volumes of activator solution which will be difficult to control. Therefore, the activator ratio will be calculated by weight.

REFERENCES

[1] European Environmental Agency, "Economic losses from climate-related extremes," 2019. https://www.eea.europa.eu/downloads/92dcd5aa70764b63b092ee9ee5777fbb/1519722091/assessment-1.

[2] P. Wallemacq and R. House, "Economic losses, poverty & disasters: 1998-2017," UNDRR and CRED. p. 31, 2018.

[3] L. Wood, "Global PET Bottle Market Report 2019: Industry Trends, Share, Size, Growth, Opportunity and Forecasts 2011-2018 & 2019-2024," Research and Markets, 2019. (Online) Available: https://www.globenewswire.com/news-release/2019/02/26/1742189/0/en/Global-PET-Bottle-Market-Report-2019-Industry-Trends-Share-Size-Growth-Opportunity-and-Forecasts-2011-2018-2019-2024.html.

[4] N. Van Chanh, B. D. Trung, and D. Van Tuan, "Recent research geopolymer concrete," Int. Conf. Asian Concr. Fed., vol. 18, pp. 235–241, 2008.

[5] V. Supraja and M. Kanta Rao, "Experimental study on geopolymer concrete incorporating GGBS," International Journal of Electronics, Communication & Soft Computing Science and Engineering, vol. 2, no. 2. pp. 11–15, 2011.

[6] C. D. Lawrence, "The production of low-energy cements," Lea's Chem. Cem. Concr, pp. 421–470, 2007.

[7] LINGL I. 10011, "Laboratory Report," 2018.

[8] EN15167-1:2006 Ground granulated blast furnace slag for use in concrete, mortar and grout. Definitions, specifications and conformity criteria.

[9] J. L. Provis and J. S. J. van Deventer, STAR 224-AAM Alkali Activated Materials. 2014.

[10] Ma'aden, "Delivering Results Responsibly, Ma'aden Annual Report," 2017.

[11] EN 196-6: 2018 "Determination of fineness and density".

[12] M. Steveson and K. Sagoe-Crentsil, "Relationships between composition, structure and strength of inorganic polymers," J. Mater. Sci., vol. 40, no. 8, pp. 2023–2036, 2005.

[13] C. A. Strydom and J. C. Swanepoel, "Utilisation of fly ash in a geopolymeric material," Appl. Geochemistry, vol. 17, no. 8, pp. 1143–1148, 2002.

[14] S. Andini, R. Cioffi, F. Colangelo, T. Grieco, F. Montagnaro, and L. Santoro, "Coal fly ash as raw material for the manufacture of geopolymer-based products," Waste Manag., vol. 28, no. 2, pp. 416–423, 2008.

[15] Liew, Y. M., Kamarudin, H., Mustafa Al Bakri, A. M., et al., "Optimization of solids-to-liquid and alkali activator ratios of calcined kaolin geopolymeric powder," Constr. Build. Mater, vol. 37, pp. 440–451, 2012.

[16] D. L. Bish and J. E. Post, Modern powder diffraction, vol. 20. Walter de Gruyter GmbH & Co KG, 2018.

[17] EN 1015-3, "Methods of Test for Mortar for Masonry." 1999.

[18] G. Li and X. Wu, "Influence of fly ash and its mean particle size on certain engineering properties of cement composite mortars," Cem. Concr. Res., vol. 35, no. 6, pp. 1128–1134, 2005.

[19] Heah, C. Y., Kamarudin, H., Al Bakri, A. M., Bnhussain, M., Luqman, M., Nizar, I. K. & Liew, Y. M. (2012) 'Study on solids-to-liquid and alkaline activator ratios on kaolin-based geopolymers', Construction and Building Materials. Elsevier Ltd, 35, pp. 912–922. doi: 10.1016/j.conbuildmat.2012.04.102.

[20] Y. M. Liew, C. Y. Heah, A. B. Mohd Mustafa, and H. Kamarudin, "Structure and properties of clay-based geopolymer cements: A review," Prog. Mater. Sci., vol. 83, pp. 595–629, 2016.

[21] X. Feng and B. Clark, "Evaluation of the physical and chemical properties of fly ash products for use in Portland cement concrete," World Coal Ash Conf., pp. 1–8, 2011.

[22] Lee, S., Seo, M. D., Kim, Y. J., Park, H. H., Kim, T. N., Hwang, Y., & Cho, S. B. "Unburned carbon removal effect on compressive strength development in a honeycomb briquette ash-based geopolymer," Int. J. Miner. Process. vol. 97, no. 1–4, pp. 20–25, 2010.

[23] A. Fernandez-Jimenez and A. Palomo, "Characterisation of fly ashes. Potential reactivity as alkaline cements," Fuel, vol. 82, pp. 2259–2265, 2003.

[24] Adam, A. "Strength and Durability Properties of Alkali Activated Slag and Fly Ash-Based Geopolymer Concrete," Chemical Engineering, no. August. p. 219, 2009.

[25] Diaz, E. I., E. N. Allouche, and Sven Eklund, "Factors affecting the suitability of fly ash as source material for geopolymers," Fuel, vol. 89, no. 5, pp. 992–996, 2010.

[26] L. M. Keyte, "Fly ash glass chemistry and inorganic polymer cements," in Geopolymers, Elsevier, 2009, pp. 15–36.

[27] Liew, Y. M., Kamarudin, H., Mustafa Al Bakri, A. M., et al. (2012b) 'Optimization of solids-to-liquid and alkali activator ratios of calcined kaolin geopolymeric powder', Construction and Building Materials. Elsevier Ltd, 37, pp. 440–451. doi: 10.1016/j.conbuildmat.2012.07.075.

[28] J. Davidovits, "Geopolymers: inorganic polymeric new materials," J. Therm. Anal., vol. 37, no. 8, pp. 1633–1656, 1991.

[29] Ha, T. H., Muralidharan, S., Bae, J. H., Ha, Y. C., Lee, H. G., Park, K. W., & Kim, D. K. "Effect of unburnt carbon on the corrosion performance of fly ash cement mortar," Constr. Build. Mater. vol. 19, no. 7, pp. 509–515, 2005.

[30] EN 196-2: 2018 "Determination of fineness and density".

[31] M. E. Nordberg, "Chemical Durability." Corning Glass Works Library: 13pp, 1964.

[32] M. Criado, A. Palomo, and A. Fernández-Jiménez, "Alkali activation of fly ashes. Part 1: Effect of curing conditions on the carbonation of the reaction products," Fuel, vol. 84, no. 16, pp. 2048–2054, 2005.

[33] Fernández-Jimenez A.; Palomo A.; Alonso M. M.; De La Torre A. G.; López-Olmo G.; Aranda M. A.G. (2006) "Quantitative determination of phases in the alkali activation of fly ash. Part I". Potential ash reactivity, Fuel, Vol: 85, Issue: 5, 625-634. DOI10.1016/j.fuel.2005.08.014.

[34] W. K. W. Lee and J. S. J. Van Deventer, "Structural reorganisation of

class F fly ash in alkaline silicate solutions," Colloids Surfaces a Physicochem. Eng. Asp, vol. 211, no. 1, pp. 49–66, 2002.

[35] R. Walker and S. Pavía, Physical properties and reactivity of pozzolans, and their influence on the properties of lime pozzolan pastes, Materials and Structures, 44, 2011, 1139 1150.

[36] T. Peters and R. Iberg, "Mineralogical changes during firing of calcium-rich brick clays," Ceram. Bull., vol. 57, no. 5, pp. 503–509, 1978.

[37] Grapes R. (2006) Pyrometamorphism. Elsevier.

[38] M. Maggetti, "Phase analysis and its significance for technology and origin," in Archaeological ceramics, 1982, pp. 121–133.

[39] R. A. Sayanam, A. K. Kalsotra, S. K. Mehta, R. S. Singh, and G. Mandal, "Studies on thermal transformations and pozzolanic activities of clay from Jammu region (India)," J. Therm. Anal., vol. 35, no. 1, pp. 99–106, 1989.

[40] I. Garcia-Lodeiro, A. Palomo, and A. Fernández-Jiménez, "An overview of the chemistry of alkali-activated cement-based binders," in Handbook of alkali-activated cements, mortars and concretes, Elsevier, 2015, pp. 19–47.

[41] EN 197-1: 2011 "Cement. Composition, specifications and conformity criteria for common cements".

[42] EN 450-1: 2012 Fly ash for concrete.

[43] P. V Krivenko, "Fly ash-alkali cements and concretes," in Proceed. 4th CANMET-ACI Intern. Conf. on Fly Ash, Silica Fume, Slag and Natural Pozzolans in Concrete, Istanbul, 1992, pp. 721–734.

[44] Komljenović M. (2015), "Mechanical strength and Young's modulus of alkali-activated cement-based binders". In: Handbook of alkali-activated Cements, mortars and concretes. Ed by F. Pacheco-Torgal, J.A. Labrincha, C. Leonelli, A. Palomo and P. Chindaprasirt. Woodhead Publishing Series in Civil and Structural Engineering. No 54. Elsevier. UK. 171-215.

[45] Pers. comm J. Reddy, Ecocem, Jan 2010.